Atmospheric Environment 165 (2017) 111–121

Contents lists available at ScienceDirect

Atmospheric Environment

journal homepage: www.elsevier.com/locate/atmosenv

Effects of canyon geometry on the distribution of traffic-related air pollution in a large urban area: Implications of a multi-canyon air pollution dispersion model

Xiangwen Fu [a], Junfeng Liu [a, *], George A. Ban-Weiss [b], Jiachen Zhang [b], Xin Huang [a], Bin Ouyang [c], Olalekan Popoola [c], Shu Tao [a]

[a] Laboratory for Earth Surface Processes, College of Urban and Environmental Sciences, Peking University, Beijing, China
[b] Department of Civil and Environmental Engineering, University of Southern California, CA, USA
[c] Department of Chemistry, University of Cambridge, Cambridge, UK

HIGHLIGHTS

- An high-resolution urban-scale traffic pollutant dispersion model is developed.
- Canyon geometry strongly influences urban pedestrian exposure to traffic pollutants.
- Building heights and street widths affect pollution inside and outside canyons.

GRAPHICAL ABSTRACT

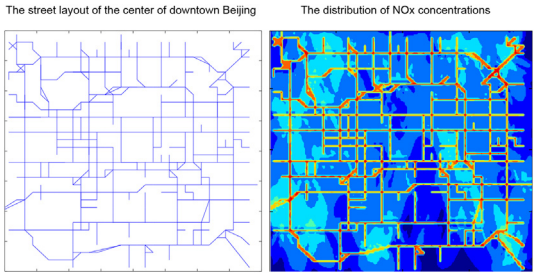

ARTICLE INFO

Article history:
Received 10 March 2017
Received in revised form
3 June 2017
Accepted 17 June 2017
Available online 21 June 2017

Keywords:
Street canyon
Canyon geometry
Traffic pollutant
Urban air pollution

ABSTRACT

Street canyons are ubiquitous in urban areas. Traffic-related air pollutants in street canyons can adversely affect human health. In this study, an urban-scale traffic pollution dispersion model is developed considering street distribution, canyon geometry, background meteorology, traffic assignment, traffic emissions and air pollutant dispersion. In the model, vehicle exhausts generated from traffic flows first disperse inside street canyons along the micro-scale wind field generated by computational fluid dynamics (CFD) model. Then, pollutants leave the street canyon and further disperse over the urban area. On the basis of this model, the effects of canyon geometry on the distribution of NO_x and CO from traffic emissions were studied over the center of Beijing. We found that an increase in building height leads to heavier pollution inside canyons and lower pollution outside canyons at pedestrian level, resulting in higher domain-averaged concentrations over the area. In addition, canyons with highly even or highly uneven building heights on each side of the street tend to lower the urban-scale air pollution concentrations at pedestrian level. Further, increasing street widths tends to lead to lower pollutant concentrations by reducing emissions and enhancing ventilation simultaneously. Our results indicate that canyon geometry strongly influences human exposure to traffic pollutants in the populated urban area. Carefully planning street layout and canyon geometry while considering traffic demand as well as local weather patterns may significantly reduce inhalation of unhealthy air by urban residents.

* Corresponding author.
E-mail address: jfliu@pku.edu.cn (J. Liu).

http://dx.doi.org/10.1016/j.atmosenv.2017.06.031
1352-2310/

1. Introduction

A street canyon refers to a narrow street with buildings built up successively along each side (Vardoulakis et al., 2003). The morphology of a street canyon hinders the dispersion of traffic pollution emissions (Hunter et al., 1992), leading to higher pedestrian exposures to pollutants inside the canyon (Pirjola et al., 2012). This may have serious deleterious human health consequences (Hertel et al., 2001). Urbanization has caused continual increases in the pervasiveness of street canyons in cities. Therefore, it is of great importance to understand the distribution of traffic-related air pollutants inside street canyons and its potential influence on human health.

Two approaches have been widely applied in street canyon studies: model simulations (computational and experimental) and field measurements. Research on model simulations usually investigate factors influencing the dispersion of pollutants (Baik and Kim, 1999) or compare performance among models (Di Sabatino et al., 2008). Field measurements usually focus on patterns of pollutant distributions in real-world street conditions (Xie et al., 2003; Zhang et al., 2012). Some studies conduct both model simulations and field measurements, mainly aimed toward validating models (Kukkonen et al., 2001; Manning et al., 2000).

Simulations of pollutant dispersion in street canyons have been performed by empirical (or semi-empirical) models and computational fluid dynamics (CFD) models (Vardoulakis et al., 2003), and they have been validated against measurements. As for empirical models, Manning et al. (2000) conducted a field experiment and examined the dependence of the performance of AEOLIUS (Assessing the Environment of Locations in Urban Streets) model on wind direction and traffic flow. The CALINE4 (California line source dispersion model, version 4) and CAR-FMI (Contaminants in the Air from a Road—Finnish Meteorological Institute) models were assessed against measurements by Levitin et al. (2005) and it was found that measured and predicted pollutant distributions agreed well for both models. The OSPM (Operational Street Pollution Model) and its adapted version simulate NO_x, CO and BC concentrations well (Aquilina and Micallef, 2004; Brasseur et al., 2015; Kukkonen et al., 2001; Lazic et al., 2016), but biases still exist in PM concentrations (Kumar et al., 2016) and the vertical gradient of pollutant distributions (Berkowicz et al., 2002). Although adopting dynamic empirical parameters improves the model performance, it has limited applicability to real-time simulation (Silver et al., 2013). ADMS-Urban (Atmospheric Dispersion Modeling System-Urban) uses the street canyon module in OSPM and has been widely used in urban air quality studies (Barnes et al., 2014; Vardoulakis et al., 2007). The model SIRANE is capable of simulating pollutant dispersion based on an urban street network, but it cannot differentiate pollutant concentrations inside a street canyon (Berrone et al., 2012; Carpentieri et al., 2012; Soulhac et al., 2016, 2011, 2012). Fallah-Shorshani et al. (2017) integrated SIRANE with a regional dispersion model and found an improved performance. Although empirical models can well predict mean concentrations, they often fail to capture the range of concentrations (Buchholz et al., 2013; Wang et al., 2016a), and their performance vary with location, time and wind conditions (Levitin et al., 2005; Vardoulakis et al., 2007; Venegas et al., 2014). Apart from empirical models, CFD models were applied in street canyon studies, including k-ε model and large eddy simulation (LES) model (Walton and Cheng, 2002; Walton et al., 2002). Solazzo et al. (2011) adopted the standard k-ε model and found that the CFD model is capable of reproducing long-term pollutant concentrations. Compared to operational models, CFD models can better resolve wind and concentration fields within street canyons with any street configuration, especially for complex building geometry (Antonioni et al., 2012; Di Sabatino et al., 2007; Murena et al., 2009; Vardoulakis et al., 2003).

Accurate pollutant dispersion simulations require precise wind flows inside street canyons, which are influenced by canyon geometry. Baik and Kim (1999) have found that the number of vortices increases with increasing canyon aspect ratio (height/width), and the distribution of pollutants in street canyons can be largely explained in terms of the vortex circulation. Small aspect ratios were found to contribute to the ventilation in street canyons as the air and pollutant exchange rates are higher when aspect ratio is smaller (Baratian-Ghorghi and Kaye, 2013; Liu et al., 2005). Moreover, other canyon geometrical factors, including canyon height ratio (the ratio of the building heights along two sides of the canyon), canyon length to height ratio, and roof shapes of upwind and downwind buildings also play an important role in air pollution dispersion (Assimakopoulos et al., 2003; Chan et al., 2001, 2003; Huang et al., 2009). In addition to single street geometry, the configuration of multiple buildings' layout (e.g. canyon contiguity, gap between buildings) also matters (Bady et al., 2011; Farrell et al., 2015; Gu et al., 2011). Aside from canyon geometry, the wind flow in street canyon is also influenced by many other factors, such as background wind speed (Solazzo et al., 2011) and wind direction (Kim and Baik, 2004), local stability conditions (Caton et al., 2003), obstacles in street canyons (Huang and Zhou, 2013), and thermal effects (Cai, 2012b; Li et al., 2012; Xie et al., 2006). Results can be sufficiently complex when different assumptions are applied (Baik et al., 2012; Gromke and Ruck, 2007; Pugh et al., 2012).

The emissions of pollutants in street canyons are mainly from motor vehicles (Huan and Kebin, 2012). Therefore, in urban areas, the traffic flow patterns also have a large impact on pollutant distributions, and the simulation of pollutant distribution in urban areas requires consideration of traffic issues. For instance, a number of studies have included traffic factors into land-use regression (LUR) models (Briggs et al., 1997; Molter et al., 2010; Tang et al., 2013). However, the LUR models are unable to characterize micro-scale pollution distribution (i.e., at the scale of tens of meters) (Hoek et al., 2008), and have to rely on extensive measurements. Other studies derived traffic emissions from traffic counts (online or extrapolated) and emission models (Buchholz et al., 2013; Lazic et al., 2016; Wang et al., 2016a). However, for an urban area consisting of hundreds to thousands of streets, it is much more difficult to derive the traffic volumes of every streets by this means compared to applying traffic assignment model. Traffic assignment determines the traffic flow pattern by the distribution of traffic demand in transportation networks (Dafermos and Sparrow, 1969). Previous research has done traffic assignment using a wide variety of methods, including modeling the variations of traffic flows and resolving individual vehicles (Kaczmarek, 2005; Nagatani, 1998; Ohazulike et al., 2013; Peng, 2013; Saumtally et al., 2011). A number of these studies have combined the process of traffic assignment with environmental pollution in urban areas. Nejadkoorki et al. (2008) modeled CO_2 emissions from traffic in a small city in the UK with SATURN (Simulation and Assignment of Traffic in Urban Road Networks). Mensink and Cosemans (2008) applied PARAMICS (PARAllel MICroscopic Simulation) to the simulation of traffic pollution and predicted pollution levels in street canyons in a city quarter in Ghent, Belgium. Xia and Shao (2005) used a Lagrangian model to simulate traffic flow and emissions, and found a good agreement between simulations and measurements.

As indicated above, the simulation of pollutant distribution in large urban areas requires the combination of street canyon effects and traffic emissions. Therefore, it is our intent to model the micro-scale distribution of traffic-induced air pollution over a large urban area using the physically-based air pollution dispersion model

considering the process of traffic assignment. In this paper, we develop a pollution dispersion model that employs simulations using a CFD model and a traffic assignment model to simulate pollutant dispersion in multiple street canyons. We further study the effects of canyon geometry on the distribution of traffic-related air pollutants over an urban area.

2. Methods

2.1. Wind field parameterization

Using CFD models to simulate pollutant distributions generates high accuracy results, but requires vast amount of computational time. Consequently, voluminous previous studies adopted CFD models for domains that cover one to a few streets. Although several CFD studies have expanded the modeling domains to an urban district or a small city (Cheshmehzangi, 2016; Gousseau et al., 2011; Kwak et al., 2015; Michioka et al., 2013; Tong et al., 2012), simulations were done only for limited runs with the consideration of computational cost. For a large urban area including thousands of streets, conducting CFD model simulations under numerous canyon geometric and meteorological scenarios is tedious, computationally expensive and time consuming. Therefore, we first characterized the wind field patterns inside a street canyon based on CFD simulations with a variety of canyon geometries and background wind configurations, and then used the characterized wind fields to calculate the dispersion of air pollutants.

A standard k-ε model was adopted to characterize turbulence, as in previous street canyon studies (Le et al., 2012; Solazzo et al., 2011). For a street, one of its two ends was determined to be the origin of a right-handed space rectangular coordinate system, and the axial direction of the street was set to be the direction of X-axis. The width of street canyon was fixed to 40 m. The settings of the input background wind profiles are as follows:

$$k(z) = 0.1V^2 \tag{1}$$

$$\varepsilon(z) = C_{\mu}^{0.75} k^{1.5} (\kappa z)^{-1} \tag{2}$$

with V representing the horizontal wind speed (m s^{-1}), z the height above ground (m), and $C_{\mu} = 0.09$, $\kappa = 0.4$.

Simulations were done for a street canyon under combinations of different values of controlling factors. The controlling factors include the aspect ratio (H/W) (when the building heights on each side of the street differ, H is set to be the average height), the canyon length to width ratio (L/W), height ratio (H_l/H_r) (H_l is the building height of the side on positive Y-axis, while H_r is the building height of the side on negative Y-axis), background wind speed (V, as in Equation (1)), and the angle between the positive X-axis and the direction to which the wind blows (α) (assuming no Z-component of background wind). The values of these factors are listed in Table S2 in the supporting information. In total, 960 (i.e., $4 \times 4 \times 5 \times 3 \times 4$) simulations were conducted.

A multiple regression analysis was employed to obtain the relationship between simulated wind fields and their controlling factors. The space inside the street canyon was proportionally divided into 7220 cells (X-direction: 20 grids, Y-direction: 19 grids, Z-direction: 19 grids). The dependent variables are the X, Y, Z-components of the average wind speed (v_x, v_y, v_z) in these cells, while the independent variables are H/W, L/W, H_l/H_r, the X and Y-components of background wind speed (V_x, V_y), and their cross terms, etc. The parameterization was done using the stepwise regression method, where the expressions of v_x, v_y and v_z were shown as Equations (3)–(5):

$$v_x = a_1 \times V_x + a_2 \times V_y + a_3 \times \frac{H}{W} + a_4 \times \frac{L}{W} + a_5 \times \left(\ln \frac{H_l}{H_r}\right)^2 + a_6 \tag{3}$$

$$v_y = a_1 \times V_x + a_2 \times \frac{H}{W} \times V_y + a_3 \times \frac{L}{W} \times V_y + a_4 \times \frac{H_l}{H_r} \times V_y + a_5 \times V_y + a_6 \tag{4}$$

$$v_z = a_1 \times {V_x}^2 + a_2 \times \frac{H_l}{H_r} \times V_x + a_3 \times V_x + a_4 \times \frac{H}{W} \times V_y + a_5 \times \frac{L}{W} \times V_y + a_6 \times \frac{H_l}{H_r} \times V_y + a_7 \times V_y + a_8 \times \left(\ln \frac{H_l}{H_r}\right)^2 + a_9 \tag{5}$$

R^2 and NRMSE (normalized root-mean-square error) were used to characterize the agreement between parameterized and CFD wind fields (Tables S3 and S4). The results demonstrate that Equations (3)–(5) can well explain the speed and direction of wind in most cells, especially for Equation (5). In addition, the parameterized and CFD wind fields have also been validated against wind-tunnel data (see Section S2).

We further investigated the dominant factors of v_x, v_y and v_z for all the cells. The dominant factor for a cell is the factor with the largest standardized beta coefficient among all controlling factors. For the equation of v_x, the dominant factor for all cells is V_x, which indicates that the X-component of wind speed inside a street canyon is mainly determined by the X-component of background wind speed. For the equation of v_y and v_z, situations are more complicated as the dominant factors for cells depend on the locations of the cells inside street canyon. Fig. S2 shows the dominant factors of v_y and v_z over three cross-sections at the beginning, the midst and the end of a street canyon. The situations of the midst and the end are quite similar, but are different from the beginning. As the wind at the beginning of the street canyon may be affected by the background wind to a great extent, the cross-sections of the midst and the end basically represent the dominant factors inside the street canyon. The dominant factors of v_y are V_y and $\frac{H_l}{H_r} \times V_y$, with V_y on the sides of the canyon while $\frac{H_l}{H_r} \times V_y$ near the X-axis. For v_z, the dominant factors are V_y, $\frac{H_l}{H_r} \times V_y$ and $\frac{L}{W} \times V_y$, with $\frac{H_l}{H_r} \times V_y$ on the windward side while V_y and $\frac{L}{W} \times V_y$ on the leeward side. This result suggests that the Y-component of the background wind is the main driver of the vortex inside street canyon. It also indicates that relative height has a considerable effect on v_y near the axis of street canyon and v_z on the windward side of street canyon.

2.2. Multi-street model of pollutant dispersion

In the multi-street model, the three-dimensional wind fields in all street canyons are derived based on the parameterization results at first. Then, traffic emissions by vehicles (assumed as a series of point sources at the bottom of street canyons) are calculated (see Section 2.3). Subsequently, pollutants emitted in street canyons are dispersed according to Gaussian puff model (Seinfeld and Pandis, 2006). The equation of the Gaussian puff model is as below:

$$c(x,y,z,T) = \int_0^{\infty} \frac{qdT}{(2\pi)^{\frac{3}{2}}\sigma_x(T)\sigma_y(T)\sigma_z(T)} \cdot e^{\left[-\frac{(x-x_p)^2}{2\sigma_x^2(T)} - \frac{(y-y_p)^2}{2\sigma_y^2(T)} - \frac{(z-z_p)^2}{2\sigma_z^2(T)}\right]} \quad (6)$$

with $c(x,y,z,T)$ representing the concentration at the point with coordinates (x,y,z) at time T, q the emission rate, x_p y_p, z_p the coordinates of a puff, and $\sigma_x(T)$, $\sigma_y(T)$, $\sigma_z(T)$ the variances. The values of σ_x, σ_y and σ_z are estimated based on the parameterization results of American Society of Mechanical Engineers (AMSE) (Seinfeld and Pandis, 2006).

Inside street canyons, vehicles emit an instantaneous puff at set intervals, and the movements of puffs in the parameterized wind field are simulated at the same interval of time. The puffs can enter the neighboring street canyons and continue moving, or reach the open space above canyons. When the puffs reach this open space, they will disperse over the domain following gridded background winds. As for reflections in urban terrain, we assume total reflection at the ground and walls of buildings for puffs.

Inside a street canyon, the pollutant concentration is calculated as the sum of contributions from all the puffs inside and outside the canyon. For places outside canyons, the concentration is contributed by all the puffs outside street canyons. Therefore, the pollutant concentration at any location of the domain can be estimated based on Gaussian puff equation. Given the small domain size and relatively longer lifetime of NO_x (~1day) and CO (~2month), the chemical evolutions of both NO_x and CO are currently ignored in this study and will be addressed in our follow-up research.

2.3. Traffic assignment model

Traffic emissions are dynamically determined by traffic flow patterns. Therefore, human exposure inside street canyons are also strongly influenced by traffic demand and street layout. In this study, we developed a traffic assignment model using the static Origin-Destination (OD) matrix, assuming that each traveler chooses the route with the lowest time cost, which is determined using the Dijkstra's Algorithm (Kreyszig, 2011). Traffic flows are allocated based on the method of incremental assignment (Ferland et al., 1975; Lu et al., 2008), which repeatedly applies all-or-nothing assignments until the traffic volumes on all roads reach quasi-equilibrium. The speed-flow function presented by the Bureau of Public Roads (BPR) of the USA has been widely used for research on traffic assignment (Brutti-Mairesse et al., 2012; Hu and Chen, 2014; Liu et al., 2015). The speed-flow Curve by the Metropolitan Transportation Commission (MTC) (Singh and Dowling, 1999), which is an updated version of the BPR Curve, is adopted to depict the relationship between vehicle speed and flow:

$$v = \frac{v_0}{\left[1 + 0.2 \times \left(\frac{q}{q_{max}}\right)^{10}\right]} \quad (7)$$

with q_{max} the traffic capacity of road, v_0 the free-flow speed of vehicles, and q and v the actual volume and speed of vehicles. Given the result of traffic assignment, the traffic emissions of NO_x and CO are derived by applying emission factor (EF, g/km) as a function of vehicle speed (v, km/h) for Beijing vehicles (Equations (8) and (9)), fitted from the simulations of MOBILE 6.2 model by Huang and Zhang (2014):

$$EF_{NOx} = 0.0002v^2 - 0.025v + 2.2987 \quad (8)$$

$$EF_{CO} = 46.847v^{-0.332} \quad (9)$$

This traffic assignment model provides traffic emission inputs for the multi-street model described in section 2.2.

2.4. Validation

We validated our model against observations during Nov. 20th - 21st, 2016 in a street canyon in downtown Beijing and made a comparison between our model and an operational model OSPM. The traffic contributions (simulated by the models) and the background pollution (measured by a nearby air quality station) were added up to be compared with measured data inside the canyon. Figs. 1 and 2 indicate that the dispersion model performs well in Beijing as it captures the pollution levels and diurnal variations of CO and NO_x concentrations. Table 1 lists four statistical performance measures that have been extensively used in evaluating of air quality models (Cai, 2012a; Chang and Hanna, 2004; Venegas et al., 2014). It quantitatively shows that our model performs as well as, if not better than performance to OSPM. In the future, we will use more measurements data to validate our model in more streets and in different seasons.

2.5. Experimental design

We applied our model to approximate traffic pollution over the center of downtown Beijing, China, which is delineated by “the 3rd Ring of Beijing”. As shown in Fig. S3a in the supporting information, the modeling domain is about 16 km × 16 km. Street layout was obtained from the GIS database of Beijing, including detailed coordinates of road length, width, and number of lanes. However, directly using the street network of Beijing for simulation is not necessary since many streets have low traffic volumes and their contributions are ignorable. To simplify our calculation, we divided the domain into 160 × 160 grids, where each grid covers an area of 100 m × 100 m. Then, the roads that connect the same two grids were merged into one road whose two ends are located at the centers of the two grids. By this means, the number of roads (able to pass vehicles) was reduced from 2578 to 642, but the general structure of the street network remains.

We adopted a widely-used mesoscale numerical weather prediction model WRF (Weather Research and Forecasting) (Kwak et al., 2015; Park et al., 2015; Wang et al., 2016b) to generate the background wind fields over the Beijing City (with a resolution of 4 km) in Jan., Apr., Jul. and Oct. 2014. The WRF-simulated results were validated against the observational data of the weather monitoring station at Beijing from the United States National Climatic Data Center (NCDC). Figs. S4 and S5 demonstrate that the wind speeds and directions are well simulated by WRF. The simulated wind fields were then divided into 8 groups according to the angle between true north and the dominant direction from which the wind blows (measured in a clockwise direction): (0°, 45°), (45°, 90°), (90°, 135°), (135°, 180°), (180°, 225°), (225°, 270°), (270°, 315°), (315°, 360°). Fig. S3b shows the wind rose of Beijing after this division. For simplicity, in each group the wind directions and speeds of the same grid were averaged, resulting in 8 typical background wind fields. Applying these typical wind fields, the pollutant concentrations were calculated and then averaged using weights proportional to the frequency of winds falling within the 8 groups to represent the annual average pollution distribution in Beijing. Background pollution concentrations originating from emissions outside the domain, as well as secondary pollution

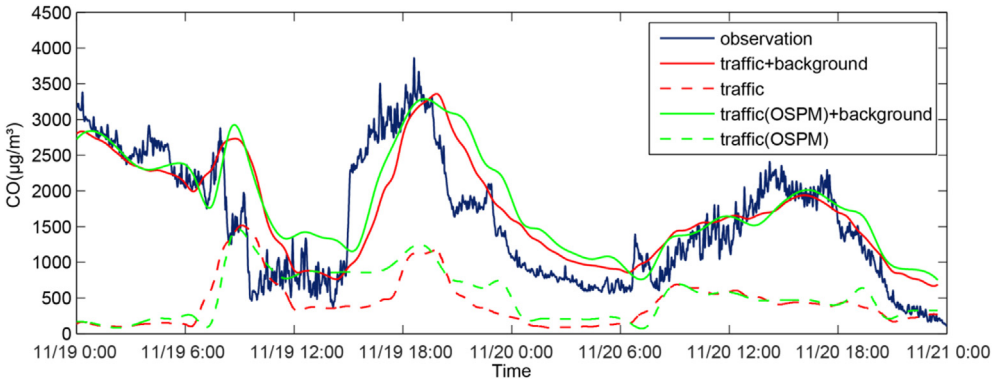

Fig. 1. The simulated and measured CO concentrations during Nov. 20th and Nov. 21st, 2016. The blue, red and green lines, respectively, represent the observed concentrations, the simulated concentrations by the dispersion model, and the simulated concentrations by OSPM. For the red and green lines, the solid lines represent the simulated concentrations with background pollution, while the dashed lines represent the simulated concentrations with traffic emissions only. (For interpretation of the references to colour in this figure legend, the reader is referred to the web version of this article.)

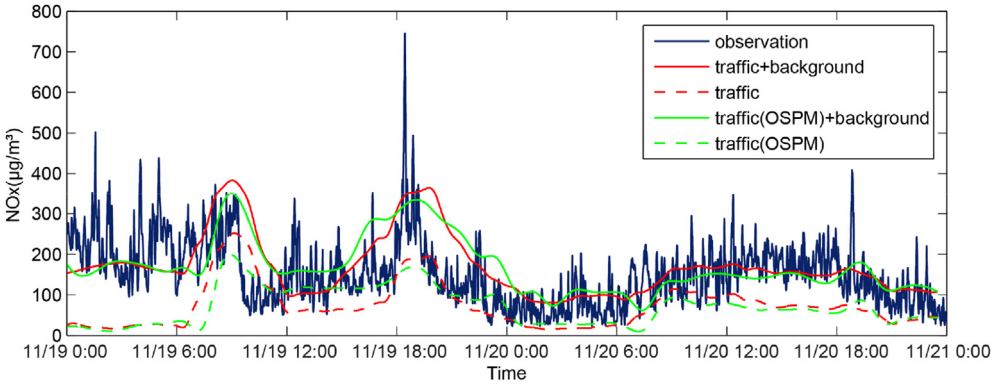

Fig. 2. Same as Fig. 1, but for NO_x concentrations.

Table 1
Summary of performance measures for model validation.

Performance measures	Definition	Ideal value	Urban criterion	Our model, CO	OSPM, CO	Our model, NO_x	OSPM, NO_x
Normalized Mean-Square Error (NMSE)	$NMSE = \overline{((C_o - C_e)^2)}/(\overline{C_o}\cdot\overline{C_e})$	0	<6	0.10	0.11	0.33	0.33
Fraction of C_e within a factor of 2 of C_o (FAC2)	Fraction where $0.5 < \frac{C_e}{C_o} < 2$	1	>0.3	0.89	0.87	0.76	0.73
Fractional Bias (FB)	$FB = 2(\overline{C_o} - \overline{C_e})/(\overline{C_o} + \overline{C_e})$	0	(-0.67, 0.67)	−0.09	−0.15	−0.11	−0.10
Correlation Coefficient (R)	$R = \overline{(C_o - \overline{C_o})(C_e - \overline{C_e})}/(\sigma_{C_o}\cdot\sigma_{C_e})$	1	–	0.81	0.82	0.39	0.34

C_o: observed concentrations, C_e: estimated concentrations, σ_{C_o}: the standard deviation of observed concentrations, σ_{C_e}: the standard deviation of estimated concentrations. Urban criteria for the performance measures are adapted from (Chang and Hanna, 2004).

sources, were ignored in this study. Pollutant concentrations over the domain at a height of 1.5 m (i.e. at pedestrian level) were archived.

In the tests on the impacts of building heights on pollutant distributions, we assumed that all buildings in the domain are of the same height, fixed at 20 m, 25 m, 30 m, 35 m, 40 m, 50 m, or 60 m. As the widths of streets differ, aspect ratios of street canyons are not uniform when a different building height is implemented. Therefore, the building height instead of the aspect ratio was investigated in this study.

To investigate the impact of height ratio, we ran multiple sensitivity tests with height ratio ranging from 0.2 to 5.0. We use the asymmetry ratio, i.e. $\gamma = |\ln(H_l/H_r)|$, to represent the degree of asymmetry of street canyons (the detailed settings are described in Section S1). For these tests, the average height of the buildings on two sides was fixed to 30 m. Therefore, pairs of building heights include (30 m, 30 m), (32 m, 28 m), (35 m, 25 m), (40 m, 20 m), (42 m, 18 m), (45 m, 15 m), (50 m, 10 m).

For the impact of street width (a parameter relevant to air pollution dispersion and traffic assignment but not affecting the street network), 5 sensitivity tests were conducted with all street widths set to be 0.5, 0.75, 1, 1.5, 2 times of the current values. The building heights were fixed to 30 m.

In all the sensitivity tests above, we adopted the “peak flow” scenario as the traffic flow pattern, where the traffic volumes per hour were set to be 750 per lane for all roads, representing the level of volume during the rush hour in Beijing (Meng et al., 2006). To examine the dependence of our results on traffic flow patterns, four additional idealized traffic scenarios were used. For each scenario, 1/3 of the “peak flow” volume is used as the base traffic flow. Additional “converging flow” is also included, which is designed to represent the travel demands of citizens going to business centers

(destinations) from different residential areas (origins). Fig. S6 shows the configuration of the eight origins (red circles) and the destinations (blue circles) of the converging flow in each scenario. 500 vehicles set off from each origin per hour and are evenly distributed to all destinations. As a consequence, the total traffic loads in the four scenarios are equal. The pollutant concentrations were simulated and compared for all scenarios.

3. Results

3.1. Pollutant distributions over the domain

Fig. 3a shows the horizontal distribution of NO_x concentrations (see Fig. S7a for CO) from traffic emissions within the domain at the pedestrian level (i.e., 1.5 m) when all building heights are set to 30 m. The distribution patterns of the two pollutants are very similar, as they share the same dispersion processes. The NO_x concentrations are about 10–100 μg m^{-3} inside street canyons, and below 1 μg m^{-3} outside the canyons. The CO concentrations are about 10 times higher than NO_x. The pollution levels inside and outside street canyons reproduced by the dispersion model differ significantly, since background pollution are not considered (note that the annual-averaged NO_2 and CO concentrations in Beijing in 2014 are 56.7 μg m^{-3} (Cheng et al., 2016b) and 1.29 mg m^{-3} (Cheng et al., 2016a)). The pollution levels in Fig. 3a should be different if having these sources included.

As shown in Fig. 3b, the domain-averaged pollutant concentrations decrease with the receptor height increases, and the rate of decrease in concentrations is slower as the receptor height increases (not for height above 15 m). Fig. 3c illustrates the probability distribution of pollutant concentrations over the domain at different heights. All curves have two peaks, representing the concentrations inside and outside street canyons. It is indicated that pollutants outside street canyons are almost evenly distributed in the vertical, while pollutants inside street canyons are typically abundant at the bottom of the canyons, resulting in a large vertical gradient.

3.2. Impacts of canyon geometry on pollutant distribution

We conducted numerous sensitivity tests with the dispersion model to study the effects of canyon geometry (building height, height ratio and width of street canyon) on the distributions of traffic-related air pollutants over the modeling domain. The results of CO are not presented if they have the same implication as NO_x.

For the impact of building height, concentrations were simulated assuming that all building heights are equal, with a value ranging from 20 m to 60 m. Fig. 4a illustrates the domain-averaged concentrations at pedestrian level, plotted against the uniform building height (H) over the domain. When H is below 40 m, the variation in domain-averaged pollutant concentrations in response to the change of H is restricted to a narrow range. However, when H is over 40 m, the domain-averaged pollutant concentrations increase remarkably as the height of building increases. According to the probability distributions of NO_x concentrations with different building heights in Fig. 4b, as H increases, the pollutant concentrations in street canyons become higher while concentrations outside the canyons become lower. The case for $H = 60$ m is slightly different, where both the concentrations inside and outside canyons increase. The trend in Fig. 4 demonstrates that higher buildings hinder the exchange of air inside and outside street canyons, leading to reduced ventilation. This is consistent with previous

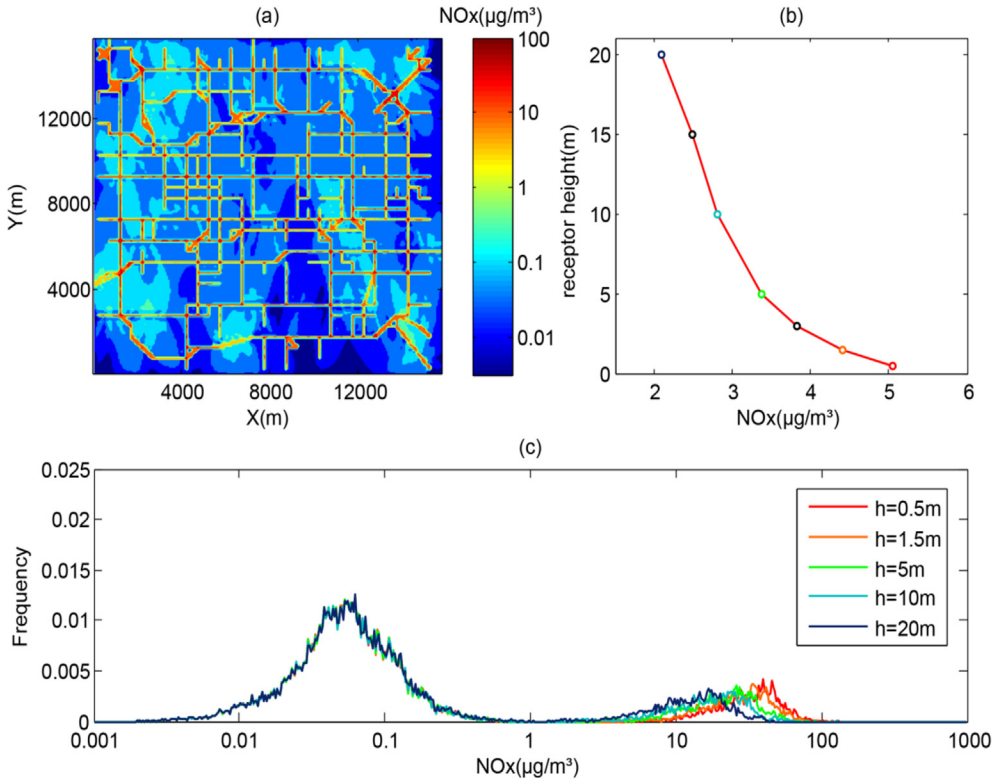

Fig. 3. (a) Distribution of NO_x concentrations at a height of 1.5 m over the center of Beijing assuming all building heights are 30 m and the traffic follows the "peak flow" pattern. (b) Domain-averaged NO_x concentrations at a receptor height of 0.5 m, 1.5 m, 3 m, 5 m, 10 m, 15 m and 20 m. (c) Probability distributions of NO_x concentrations over the domain at different receptor heights. The colors of curves in (c) are consistent with the colors of circles in (b). (For interpretation of the references to colour in this figure legend, the reader is referred to the web version of this article.)

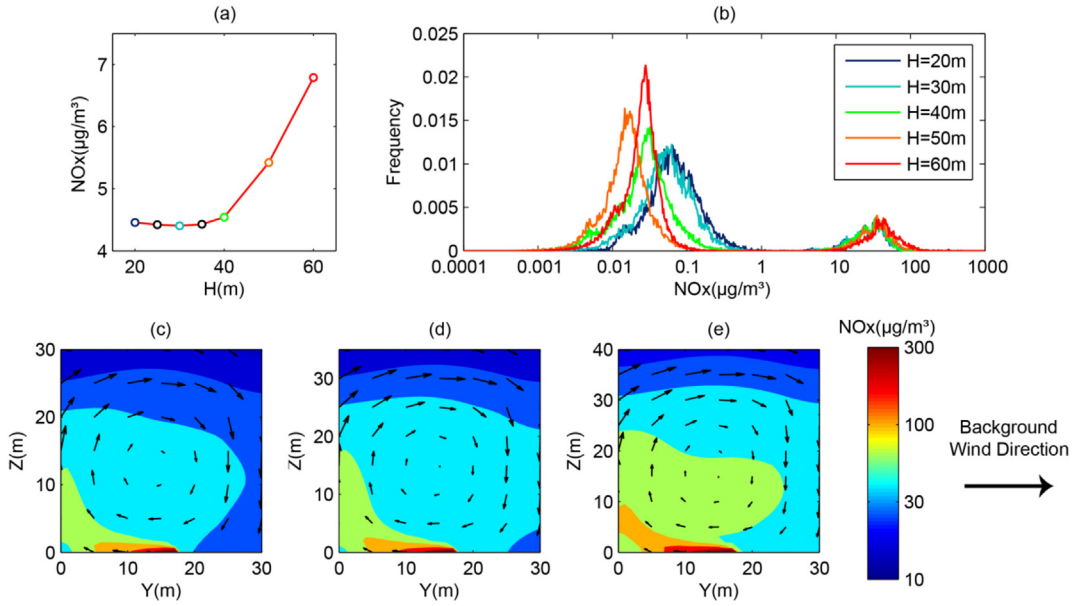

Fig. 4. (a) Domain-averaged concentrations of NO_x at a height of 1.5 m with uniform building height set to be 20 m, 25 m, 30 m, 35 m, 40 m, 50 m, and 60 m. (b) Probability distributions of NO_x concentrations over the domain at a height of 1.5 m with different uniform building heights. The colors of curves in (b) are consistent with the colors of circles in (a). (c–e) The transverse wind fields (arrows) and NO_x concentrations (color contours) over the center cross-sections of three symmetric street canyons with different aspect ratios. The length and width of the canyons are 160 m and 30 m, respectively. The building heights on both sides of the canyons are (c) 30 m, (d) 35 m, and (e) 40 m. The background wind is set to 3 m s^{-1}. Note that the vertical axis range differs for each panel. (For interpretation of the references to colour in this figure legend, the reader is referred to the web version of this article.)

findings (Liu et al., 2005), in which large eddy simulation (LES) of pollutant dispersion inside a single street was investigated. As shown in Fig. S8, a clockwise vortex appears in all canyons and wind flow is stronger above a height of 5 m. However, near the ground level (i.e., below 5 m), wind speed is typically smaller and is even lower in a canyon with greater aspect ratio. This inhibits the ventilation of traffic pollutants, which are usually emitted by vehicles below 1 m. Consequently, air pollutants are more likely to be trapped at the leeward side of the bottom of a deeper street canyon (Fig. 4c–e).

Fig. 5a demonstrates the domain-averaged concentrations of NO_x against asymmetry ratio, γ. For γ between 0 and 0.85 (i.e., height ratio varies between 0.43 and 2.33), as the street canyon becomes more asymmetric, the domain-averaged pollutant concentration decreases slightly at first and then increases. The pollutant concentration shows a peak where γ reaches 0.85 (i.e., with a corresponding height ratio of 0.43 or 2.33). For the highly asymmetric case where γ is above 0.85 (i.e., height ratio is below 0.43 or above 2.33), pollutant concentration becomes lower as the street canyon becomes more asymmetric. As shown in Figs. S9 and S10, wind turbulence inside the canyon and thus the distribution of pollutant inside and outside the canyon change substantially with different height ratios and background wind directions. When the building on the leeward side is lower than that of the windward side, pollutants emitted at the bottom of canyons tend to disperse outside the canyon. In contrast, when the windward building is lower, pollutants are more likely to accumulate inside the canyons, except for the highly asymmetric case where pollutant concentrations inside canyon are low due to the disappearance of geometric features of street canyon (Fig. S10f). According to Fig. 5b, under the wind fields applied in the simulation the pollutants are prone to disperse outside canyons when the canyons are asymmetric, raising air pollution levels outside canyons while lowering pollution levels inside canyons. Hence, the variation of the domain-averaged concentration at pedestrian level with γ is a joint effect of the concentration changes inside and outside canyons.

Besides building height and height ratio, street width can have multiple effects on pollution distribution. Firstly, traffic capacity

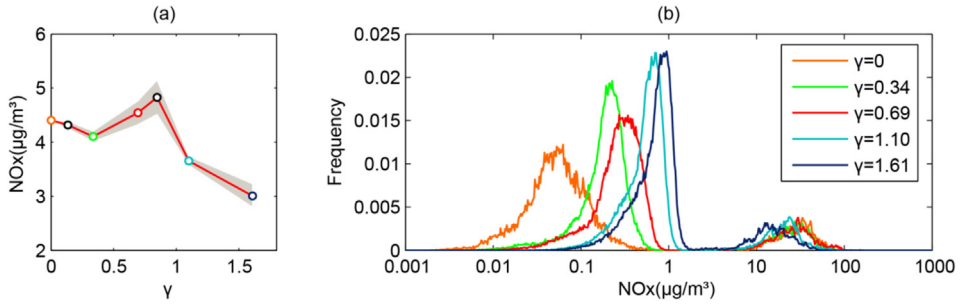

Fig. 5. (a) Domain-averaged concentrations of NO_x at a height of 1.5 m with different asymmetry ratio $\gamma = |\ln(H_l/H_r)|$. The values of γ are set to be 0, 0.13, 0.34, 0.69, 0.85, 1.10, and 1.61. The red line is the average result of four possible height ratio scenarios with the same γ value, while the grey shade defines the range. (b) Probability distributions of NO_x concentrations over the domain at a height of 1.5 m with different γ (only the average result of different height ratio scenarios is shown). The colors of curves in (b) are consistent with the colors of circles in (a). (For interpretation of the references to colour in this figure legend, the reader is referred to the web version of this article.)

and congestion of roadways, and thus traffic emissions, are partly determined by street width. Secondly, increasing the width of a street canyon reduces its aspect ratio and promotes ventilation, lowering pollutant concentrations. Fig. 6 illustrates the changes of NO_x concentrations (Fig. S11 for CO) with street widths ranging from 0.5 to 2 times the current value. When the street widths are larger, pollutant concentrations inside and outside street canyons both show a significant downward trend. The domain-averaged NO_x and CO concentrations even drop by 90% and 95% when street widths are widened from 0.5 to 2 times of the original case. The difference in changes between the two species arises from their emission factors (Equations (8) and (9)), where CO emissions are more sensitive to vehicle speed.

3.3. Caveats

Here we summarize the uncertainties associated with the modeling results. Firstly, we assume that all buildings are successively along the road, while in reality there are multiple openings on the walls of a street canyon, where polluted air may leak out of the street. This simplification could potentially overestimate the simulated pollutant concentrations inside street canyons, but underestimate pollution levels outsides the streets. Secondly, due to the lack of data on building heights and traffic volumes, assumed building heights are instead adopted for simulations and a traffic assignment model is used rather than online or extrapolated traffic counts. When examining the robustness of results under different traffic flow patterns, as the traffic demands are complex and difficult to determine, the OD matrices are also idealized. Therefore, the distributions of pollutants do not reflect the real conditions, but rather a theoretical characterization of the impacts of canyon geometry. To test the dependence of our results on traffic flow patterns, we have conducted parallel tests with the four traffic scenarios described in section 2.5. Our tests indicate that although pollutant concentrations differ between scenarios, our findings are robust. For example, Figs. S12–S15 demonstrate that the changes of domain-averaged NO_x concentrations at pedestrian level with building height are similar to the result of the "peak flow" scenario when the traffic flows follow scenarios 1–4. Thirdly, in the dispersion model, the treatments of dispersion parameters and reflections of Gaussian puffs also bring uncertainties to pollutant distribution in complex urban terrains. Moreover, the parameterization of CFD wind fields may not apply to extreme cases of canyon geometry that lie far beyond the parameter space. We will use CFD simulations directly for these extreme cases as they appear much less frequently in urban area. In addition, we did not take into account the effects of chemical processes, which may lead to biases when NO_x is converted to other NO_y species, or CO is chemically converted from other volatile organic compounds (VOCs).

Even with those uncertainties, the prediction of our model agrees well with the street-level observations. In the future, we will further improve the model to address these uncertainties, and allow our model configuration to more realistically represent the conditions over the center of Beijing. We will also collect more street-level measurement data to further optimize model parameters.

4. Discussion and conclusion

In this study, we examine the effects of street canyon geometry on air pollutant distributions over the center of downtown Beijing. We first parameterized the wind field inside a street canyon on the basis of simulations using a CFD model, and then developed an urban-scale traffic pollutant dispersion model that represents street distributions, canyon geometries, background meteorology, traffic assignment, traffic emissions and air pollutant dispersion. After validation of the dispersion model against measurement data, the distributions of traffic-related air pollutants at pedestrian level over the downtown area of Beijing were then modeled under a variety of canyon geometry configurations.

For the impact of building height on pollutant concentrations, we found that higher buildings hinder ventilation in street canyons, resulting in higher pollutant concentrations inside street canyons and lower pollution outside the canyons. The increase of building height from 20 m to 40 m has little influence on pollutant concentrations. However, when building height is over 40 m, the pollutant concentrations within the street canopy increase rapidly as the building height increases. The height of a six-floor building is approximately 20 m, consistent with the height of many old buildings in Beijing. As the building heights in Beijing are consistently growing during urbanization (Cheng et al., 2011), in the future, it is possible that most buildings in central Beijing would reach 60 m. As the model results imply, if building height is increased from 20 m to 60 m, the domain-averaged traffic-related NO_x and CO concentrations could increase by about 52%. This means that human exposure to air pollutants in Beijing could increase even with fixed traffic emissions. What is more, emissions from road transport are bound to increase due to rapid vehicle growth in cities of China (Zheng et al., 2014). Therefore, policymakers on urban planning should pay special attention to the height of buildings in order to prevent increasing surface air pollution caused by traffic emissions.

We also found that uneven building heights along a street affect pollutant dispersion significantly. For street canyons with a height ratio approaching 0.43 or 2.33, the highest domain-averaged pollution level is observed. When relatively high or relatively low canyon height ratio is reached, the concentration becomes lower. Therefore, lower concentrations at pedestrian level appear when

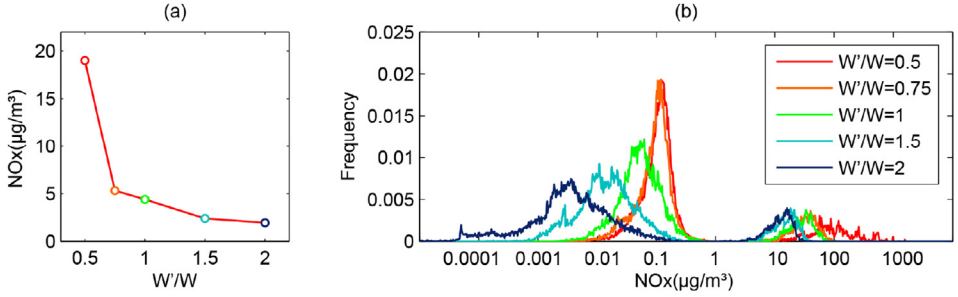

Fig. 6. (a) Domain-averaged concentrations of NO_x at a height of 1.5 m with street widths set to be 0.5, 0.75, 1, 1.5, 2 times (W'/W) of the current values. (b) Probability distributions of NO_x concentrations over the domain at a height of 1.5 m with different street widths. All building heights are set to be 30 m. The colors of curves in (b) are consistent with the colors of circles in (a). (For interpretation of the references to colour in this figure legend, the reader is referred to the web version of this article.)

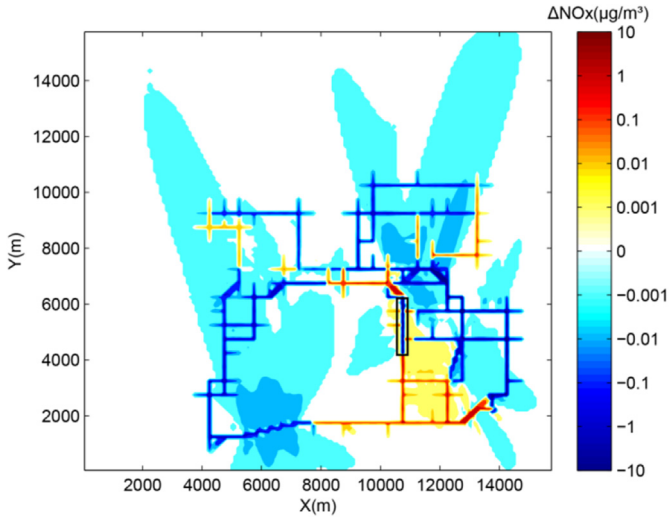

Fig. 7. The variations of NO_x concentrations over the domain at a height of 1.5 m after doubling the width of a street shown by the black rectangle. All building heights are set to be 30 m. The traffic flows follow scenario 1.

highly symmetric or highly asymmetric street canyons are applied in the urban area. This result indicates that carefully planning the asymmetry ratio could help lower the overall exposure of humans to air pollutants.

What is more, increasing street widths result in lower pollutant concentrations by reducing emissions (e.g., NO_x emissions drop by 29% (57% for CO) when street widths are 2 times the current values) and enhancing ventilation simultaneously. In reality, it is difficult to expand the widths of all streets in an urban area, but may only improve the road capacity where has the severest traffic jam. Fig. 7 shows the pollution changes when a road with large traffic volume and heavy pollution (see Fig. S16 for the base, the target street is marked with a black rectangle) is widened by a factor of 2. Apart from the sharp decline of pollutant concentrations inside this street canyon, this reconstruction would alter concentrations in a number of street canyons because of the change of traffic flow patterns. This indicates that widening a street has a considerable mitigation effect on its air quality, but the effect on other parts of the urban area varies from place to place. To evaluate the overall net health impact over the entire area, it needs to incorporate population distribution into this analysis, which will be evaluated in follow-up research.

In summary, air pollution from road transport in cities remains a great challenge to urban environmental management (Kelly and Zhu, 2016). Canyon geometry and street layout have apparent impacts on traffic-induced air pollution at pedestrian level in urban areas. To achieve the goal of reducing the damage from traffic-related air pollution to human health, besides mitigation of vehicle emissions, canyon geometry should be deliberately considered and optimized during the process of urban planning.

Acknowledgements

The author thanks J. Meng, W. Tao, Z. Chen, J. Xu, K. Yi, H. Feng, X. Hu and Z. Li for their sincere support to this study. This work was supported by funding from the National Key Research and Development Program of China [NO. 2016YFC0206202]; the National Natural Science Foundation of China [grant number 41671491, 41571130010, and 41390240]; the 111 Project [B14001]; and the undergraduate student research training program.

Appendix A. Supplementary data

Supplementary data related to this article can be found at http://dx.doi.org/10.1016/j.atmosenv.2017.06.031.

References

Antonioni, G., Burkhart, S., Burman, J., Dejoan, A., Fusco, A., Gaasbeek, R., Gjesdal, T., Jappinen, A., Riikonen, K., Morra, P., Parrnhed, O., Santiago, J.L., 2012. Comparison of CFD and operational dispersion models in an urban-like environment. Atmos. Environ. 47, 365–372.
Aquilina, N., Micallef, A., 2004. Evaluation of the operational street pollution model using data from European cities. Environ. Monit. Assess. 95, 75–96.
Assimakopoulos, V.D., ApSimon, H.M., Moussiopoulos, N., 2003. A numerical study of atmospheric pollutant dispersion in different two-dimensional street canyon configurations. Atmos. Environ. 37, 4037–4049.
Bady, M., Kato, S., Takahashi, T., Huang, H., 2011. An experimental investigation of the wind environment and air quality within a densely populated urban street canyon. J. Wind Eng. Industrial Aerodynamics 99, 857–867.
Baik, J.J., Kim, J.J., 1999. A numerical study of flow and pollutant dispersion characteristics in urban street canyons. J. Appl. Meteorology 38, 1576–1589.
Baik, J.J., Kwak, K.H., Park, S.B., Ryu, Y.H., 2012. Effects of building roof greening on air quality in street canyons. Atmos. Environ. 61, 48–55.
Baratian-Ghorghi, Z., Kaye, N.B., 2013. The effect of canyon aspect ratio on flushing of dense pollutants from an isolated street canyon. Sci. Total Environ. 443, 112–122.
Barnes, M.J., Brade, T.K., MacKenzie, A.R., Whyatt, J.D., Carruthers, D.J., Stocker, J., Cai, X., Hewitt, C.N., 2014. Spatially-varying surface roughness and ground-level air quality in an operational dispersion model. Environ. Pollut. 185, 44–51.
Berkowicz, R., Ketzel, M., Vachon, G., Louka, P., Rosant, J.M., Mestayer, P.G., Sini, J.F., 2002. Examination of traffic pollution distribution in a street canyon using the Nantes'99 experimental data and comparison with model results. Urban Air Qual. - Recent Adv. Proc. 311–324.
Berrone, S., De Santi, F., Pieraccini, S., Marro, M., 2012. Coupling traffic models on networks and urban dispersion models for simulating sustainable mobility strategies. Comput. Math. Appl. 64, 1975–1991.
Brasseur, O., Declerck, P., Heene, B., Vanderstraeten, P., 2015. Modelling Black Carbon concentrations in two busy street canyons in Brussels using CANS(BC). Atmos. Environ. 101, 72–81.
Briggs, D.J., Collins, S., Elliott, P., Fischer, P., Kingham, S., Lebret, E., Pryl, K., VAnReeuwijk, H., Smallbone, K., VanderVeen, A., 1997. Mapping urban air pollution using GIS: a regression-based approach. Int. J. Geogr. Inf. Sci. 11, 699–718.
Brutti-Mairesse, E., Teillac, S., Andree, M., Leclercq, L., 2012. Estimation of pollutant emissions from the road traffic at a city scale, and its sensitivity as regards the calibration of the static traffic assignment models. Transp. Res. Arena 2012 (48), 2091–2100.
Buchholz, S., Krein, A., Junk, J., Heinemann, G., Hoffmann, L., 2013. Simulation of urban-scale air pollution patterns in Luxembourg: contributing sources and emission scenarios. Environ. Model. Assess. 18, 271–283.
Cai, X.M., 2012a. Effects of differential wall heating in street canyons on dispersion and ventilation characteristics of a passive scalar. Atmos. Environ. 51, 268–277.
Cai, X.M., 2012b. Effects of wall heating on flow characteristics in a street canyon. Boundary-Layer Meteorol. 142, 443–467.
Carpentieri, M., Salizzoni, P., Robins, A., Soulhac, L., 2012. Evaluation of a neighbourhood scale, street network dispersion model through comparison with wind tunnel data. Environ. Model. Softw. 37, 110–124.
Caton, F., Britter, R.E., Dalziel, S., 2003. Dispersion mechanisms in a street canyon. Atmos. Environ. 37, 693–702.
Chan, A.T., Au, W.T.W., So, E.S.P., 2003. Strategic guidelines for street canyon geometry to achieve sustainable street air quality - part II: multiple canopies and canyons. Atmos. Environ. 37, 2761–2772.
Chan, A.T., So, E.S.P., Samad, S.C., 2001. Strategic guidelines for street canyon geometry to achieve sustainable street air quality. Atmos. Environ. 35, 4089–4098.
Chang, J.C., Hanna, S.R., 2004. Air quality model performance evaluation. Meteorology Atmos. Phys. 87, 167–196.
Cheng, F., Wang, C., Wang, J.L., Tang, F.X., Xi, X.H., 2011. Trend analysis of building height and total floor space in Beijing, China using ICESat/GLAS data. Int. J. Remote Sens. 32, 8823–8835.
Cheng, N.L., Chen, T., Zhang, D.W., Li, Y.T., Dong, X., Wang, X., Huan, N., Chen, C., Meng, F., 2016a. Spatial and Temporal Distribution of CO During 2013–2014 in Beijing. Environ. Sci. Technol. 39, 150–155.
Cheng, N.L., Li, Y.T., Chen, T., Zhang, D.W., Dong, X., Wang, X., Huan, N., Liu, B.X., Yan, H., Meng, F., 2016b. Spatial and temporal distribution of NO2 during 2013-2014 in Beijing. China Environ. Sci. 36, 18–26.
Cheshmehzangi, A., 2016. Multi-spatial environmental performance evaluation towards integrated urban design: a procedural approach with computational simulations. J. Clean. Prod. 139, 1085–1093.
Dafermos, S.C., Sparrow, F.T., 1969. Traffic assignment problem for a general network. JOURNAL OF RESEARCH of the National Bureau of standards - B. Math. Sci. 73B, 91–118.
Di Sabatino, S., Buccolieri, R., Pulvirenti, B., Britter, R., 2007. Simulations of pollutant

dispersion within idealised urban-type geometries with CFD and integral models. Atmos. Environ. 41, 8316–8329.
Di Sabatino, S., Buccolieri, R., Pulvirenti, B., Britter, R.E., 2008. Flow and pollutant dispersion in street canyons using FLUENT and ADMS-Urban. Environ. Model. Assess. 13, 369–381.
Fallah-Shorshani, M., Shekarrizfard, M., Hatzopoulou, M., 2017. Integrating a street-canyon model with a regional Gaussian dispersion model for improved characterisation of near-road air pollution. Atmos. Environ. 153, 21–31.
Farrell, W.J., Cavellin, L.D., Weichenthal, S., Goldberg, M., Hatzopoulou, M., 2015. Capturing the urban canyon effect on particle number concentrations across a large road network using spatial analysis tools. Build. Environ. 92, 328–334.
Ferland, J.A., Florian, M., Achim, C., 1975. On incremental methods for traffic assignment. Transp. Res. 9, 237–239.
Gousseau, P., Blocken, B., Stathopoulos, T., van Heijst, G.J.F., 2011. CFD simulation of near-field pollutant dispersion on a high-resolution grid: a case study by LES and RANS for a building group in downtown Montreal. Atmos. Environ. 45, 428–438.
Gromke, C., Ruck, B., 2007. Influence of trees on the dispersion of pollutants in an urban street canyon - experimental investigation of the flow and concentration field. Atmos. Environ. 41, 3287–3302.
Gu, Z.L., Zhang, Y.W., Cheng, Y., Lee, S.C., 2011. Effect of uneven building layout on air flow and pollutant dispersion in non-uniform street canyons. Build. Environ. 46, 2657–2665.
Hertel, O., De Leeuw, F.A.A.M., Raaschou-Nielsen, O., Jensen, S.S., Gee, D., Herbarth, O., Pryor, S., Palmgren, F., Olsen, E., 2001. Human exposure to outdoor air pollution (IUPAC technical report). Pure Appl. Chem. 73, 933–958.
Hoek, G., Beelen, R., de Hoogh, K., Vienneau, D., Gulliver, J., Fischer, P., Briggs, D., 2008. A review of land-use regression models to assess spatial variation of outdoor air pollution. Atmos. Environ. 42, 7561–7578.
Hu, C., Chen, W., 2014. Synthesis for static multi-path traffic assignment models. Mod. Transp. Technol. 01, 65–68.
Huan, L., Kebin, H., 2012. Traffic optimization: a new way for air pollution control in China's urban areas. Environ. Sci. Technol. 46, 5660–5661.
Huang, Y., Zhang, Q., 2014. Influence of driving speed on vehicle emission factors in Beijing. Transp. Stand. 24, 102–106.
Huang, Y.D., Hu, X.N., Zeng, N.B., 2009. Impact of wedge-shaped roofs on airflow and pollutant dispersion inside urban street canyons. Build. Environ. 44, 2335–2347.
Huang, Y.D., Zhou, Z.H., 2013. A numerical study of airflow and pollutant dispersion inside an urban street canyon containing an elevated expressway. Environ. Model. Assess. 18, 105–114.
Hunter, L.J., Johnson, G.T., Watson, I.D., 1992. An investigation of 3-dimensional characteristics of flow regimes within the urban canyon. Atmos. Environ. Part B-Urban Atmos. 26, 425–432.
Kaczmarek, M., 2005. Fuzzy group model of traffic flow in street networks. Transp. Res. Part C-Emerging Technol. 13, 93–105.
Kelly, F.J., Zhu, T., 2016. Transport solutions for cleaner air. Science 352, 934–936.
Kim, J.J., Baik, J.J., 2004. A numerical study of the effects of ambient wind direction on flow and dispersion in urban street canyons using the RNG k-epsilon turbulence model. Atmos. Environ. 38, 3039–3048.
Kreyszig, E., 2011. Advanced Engineering Mathematics, tenth ed. John Wiley & Sons Inc.
Kukkonen, J., Valkonen, E., Walden, J., Koskentalo, T., Aarnio, P., Karppinen, A., Berkowicz, R., Kartastenpaa, R., 2001. A measurement campaign in a street canyon in Helsinki and comparison of results with predictions of the OSPM model. Atmos. Environ. 35, 231–243.
Kumar, A., Ketzel, M., Patil, R.S., Dikshit, A.K., Hertel, O., 2016. Vehicular pollution modeling using the operational street pollution model (OSPM) for Chembur, Mumbai (India). Environ. Monit. Assess. 188.
Kwak, K.H., Baik, J.J., Ryu, Y.H., Lee, S.H., 2015. Urban air quality simulation in a high-rise building area using a CFD model coupled with mesoscale meteorological and chemistry-transport models. Atmos. Environ. 100, 167–177.
Lazic, L., Urosevic, M.A., Mijic, Z., Vukovic, G., Ilic, L., 2016. Traffic contribution to air pollution in urban street canyons: integrated application of the OSPM, moss biomonitoring and spectral analysis. Atmos. Environ. 141, 347–360.
Le, W., Yun-wei, Z., Zhao-lin, G., 2012. The numerical simulation of pollutant dispersion in street canyons under dynamic wind field and traffic flux conditions. China Environ. Sci. 32, 2161–2167.
Levitin, J., Harkonen, J., Kukkonen, J., Nikmo, J., 2005. Evaluation of the CALINE4 and CAR-FMI models against measurements near a major road. Atmos. Environ. 39, 4439–4452.
Li, X.X., Britter, R.E., Norford, L.K., Koh, T.Y., Entekhabi, D., 2012. Flow and pollutant transport in urban street canyons of different aspect ratios with ground heating: large-eddy simulation. Boundary-Layer Meteorol. 142, 289–304.
Liu, C.H., Leung, D.Y.C., Barth, M.C., 2005. On the prediction of air and pollutant exchange rates in street canyons of different aspect ratios using large-eddy simulation. Atmos. Environ. 39, 1567–1574.
Liu, L., Hwang, T., Lee, S., Ouyang, Y.F., Lee, B., Smith, S.J., Yan, F., Daenzer, K., Bond, T.C., 2015. Emission projections for long-haul freight trucks and rail in the United States through 2050. Environ. Sci. Technol. 49, 11569–11576.
Lu, H., Qin, X., Ma, H., 2008. Comparison research of several traffic assignment methods. Highw. Eng. 05, 48–51.
Manning, A.J., Nicholson, K.J., Middleton, D.R., Rafferty, S.C., 2000. Field study of wind and traffic to test a street canyon pollution model. Environ. Monit. Assess. 60, 283–313.
Meng, J., Fu, H., ZHao, X., Zhang, W., Song, M., 2006. The investigation and analyze of the third Ring's transportation situation in Beijing. J. Cap. Normal Univ. Nat. Sci. Ed. 27, 89–92.
Mensink, C., Cosemans, G., 2008. From traffic flow simulations to pollutant concentrations in street canyons and backyards. Environ. Model. Softw. 23, 288–295.
Michioka, T., Sato, A., Sada, K., 2013. Large-eddy simulation coupled to mesoscale meteorological model for gas dispersion in an urban district. Atmos. Environ. 75, 153–162.
Molter, A., Lindley, S., de Vocht, F., Simpson, A., Agius, R., 2010. Modelling air pollution for epidemiologic research - Part I: a novel approach combining land use regression and air dispersion. Sci. Total Environ. 408, 5862–5869.
Murena, F., Favale, G., Vardoulakis, S., Solazzo, E., 2009. Modelling dispersion of traffic pollution in a deep street canyon: application of CFD and operational models. Atmos. Environ. 43, 2303–2311.
Nagatani, T., 1998. Modified KdV equation for jamming transition in the continuum models of traffic. Phys. A 261, 599–607.
Nejadkoorki, F., Nicholson, K., Lake, I., Davies, T., 2008. An approach for modelling CO(2) emissions from road traffic in urban areas. Sci. Total Environ. 406, 269–278.
Ohazulike, A.E., Still, G., Kern, W., van Berkum, E.C., 2013. An origin-destination based road pricing model for static and multi-period traffic assignment problems. Transp. Res. Part E-Logistics Transp. Rev. 58, 1–27.
Park, S.B., Baik, J.J., Lee, S.H., 2015. Impacts of mesoscale wind on turbulent flow and ventilation in a densely built-up urban area. J. Appl. Meteorology Climatol. 54, 811–824.
Peng, G.H., 2013. A new lattice model of traffic flow with the consideration of individual difference of anticipation driving behavior. Commun. Nonlinear Sci. Numer. Simul. 18, 2801–2806.
Pirjola, L., Lahde, T., Niemi, J.V., Kousa, A., Ronkko, T., Karjalainen, P., Keskinen, J., Frey, A., Hillamo, R., 2012. Spatial and temporal characterization of traffic emissions in urban microenvironments with a mobile laboratory. Atmos. Environ. 63, 156–167.
Pugh, T.A.M., MacKenzie, A.R., Whyatt, J.D., Hewitt, C.N., 2012. Effectiveness of green infrastructure for improvement of air quality in urban street canyons. Environ. Sci. Technol. 46, 7692–7699.
Saumtally, T., Lebacque, J.P., Haj-Salem, H., 2011. Static traffic assignment with side constraints in a dense orthotropic network. State Art Eur. Quantitative Oriented Transp. Logist. Res. 2011, 20.
Seinfeld, J., Pandis, S., 2006. Atmospheric Chemistry and Physics, second ed. John Wiley & Sons, INC, Hoboken, New Jersey.
Silver, J.D., Ketzel, M., Brandt, J., 2013. Dynamic parameter estimation for a street canyon air quality model. Environ. Model. Softw. 47, 235–252.
Singh, R., Dowling, R., 1999. Improved Speed-flow Relationships: Application to Transportation Planning Models. Paper presented at the Seventh TRB Conference on the Application of Transportation Planning Methods, pp. 340–349.
Solazzo, E., Vardoulakis, S., Cai, X.M., 2011. A novel methodology for interpreting air quality measurements from urban streets using CFD modelling. Atmos. Environ. 45, 5230–5239.
Soulhac, L., Lamaison, G., Cierco, F.X., Ben Salem, N., Salizzoni, P., Mejean, P., Armand, P., Patryl, L., 2016. SIRANERISK: modelling dispersion of steady and unsteady pollutant releases in the urban canopy. Atmos. Environ. 140, 242–260.
Soulhac, L., Salizzoni, P., Cierco, F.X., Perkins, R., 2011. The model SIRANE for atmospheric urban pollutant dispersion; part I, presentation of the model. Atmos. Environ. 45, 7379–7395.
Soulhac, L., Salizzoni, P., Mejean, P., Didier, D., Rios, I., 2012. The model SIRANE for atmospheric urban pollutant dispersion; PART II, validation of the model on a real case study. Atmos. Environ. 49, 320–337.
Tang, R., Blangiardo, M., Gulliver, J., 2013. Using building heights and street configuration to enhance intraurban PM10, NOX, and NO2 land use regression models. Environ. Sci. Technol. 47, 11643–11650.
Tong, Z.M., Wang, Y.J., Patel, M., Kinney, P., Chrirud, S., Zhang, K.M., 2012. Modeling spatial variations of black carbon particles in an urban highway-building environment. Environ. Sci. Technol. 46, 312–319.
Vardoulakis, S., Fisher, B.E.A., Pericleous, K., Gonzalez-Flesca, N., 2003. Modelling air quality in street canyons: a review. Atmos. Environ. 37, 155–182.
Vardoulakis, S., Valiantis, M., Milner, J., ApSimon, H., 2007. Operational air pollution modelling in the UK - street canyon applications and challenges. Atmos. Environ. 41, 4622–4637.
Venegas, L.E., Mazzeo, N.A., Dezzutti, M.C., 2014. A simple model for calculating air pollution within street canyons. Atmos. Environ. 87, 77–86.
Walton, A., Cheng, A.Y.S., 2002. Large-eddy simulation of pollution dispersion in an urban street canyon - Part II: idealised canyon simulation. Atmos. Environ. 36, 3615–3627.
Walton, A., Cheng, A.Y.S., Yeung, W.C., 2002. Large-eddy simulation of pollution dispersion in an urban street canyon - Part I: comparison with field data. Atmos. Environ. 36, 3601–3613.
Wang, A., Fallah-Shorshani, M., Xu, J.S., Hatzopoulou, M., 2016a. Characterizing near-road air pollution using local-scale emission and dispersion models and validation against in-situ measurements. Atmos. Environ. 142, 452–464.
Wang, Q.Y., Huang, R.J., Cao, J.J., Tie, X.X., Shen, Z.X., Zhao, S.Y., Han, Y.M., Li, G.H., Li, Z.Q., Ni, H.Y., Zhou, Y.Q., Wang, M., Chen, Y., Su, X.L., 2016b. Contribution of regional transport to the black carbon aerosol during winter haze period in Beijing. Atmos. Environ. 132, 11–18.
Xia, L.P., Shao, Y.P., 2005. Modelling of traffic flow and air pollution emission with

application to Hong Kong Island. Environ. Model. Softw. 20, 1175–1188.
Xie, S.D., Zhang, Y.H., Li, Q., Tang, X.Y., 2003. Spatial distribution of traffic-related pollutant concentrations in street canyons. Atmos. Environ. 37, 3213–3224.
Xie, X.M., Liu, C.H., Leung, D.Y.C., Leung, M.K.H., 2006. Characteristics of air exchange in a street canyon with ground heating. Atmos. Environ. 40, 6396–6409.
Zhang, Y.W., Gu, Z.L., Cheng, Y., Shen, Z.X., Dong, J.G., Lee, S.C., 2012. Measurement of diurnal variations of PM2.5 mass concentrations and factors affecting pollutant dispersion in urban street canyons under weak-wind conditions in Xi'an. Aerosol Air Qual. Res. 12, 1261–1268.
Zheng, B., Huo, H., Zhang, Q., Yao, Z.L., Wang, X.T., Yang, X.F., Liu, H., He, K.B., 2014. High-resolution mapping of vehicle emissions in China in 2008. Atmos. Chem. Phys. 14, 9787–9805.